Preparation of Nitro-Phenothiazine Based Oxime Esters (OXEs) as Dual Photo/Thermal Initiators for 3D Printing

Xiaoxiang Zhang, Xiaotong Peng, Di Zhu, Yijun Zhang, Marie Le Dot, Serife Ozen, Michael Schmitt, Fabrice Morlet-Savary, Pu Xiao, Frédéric Dumur, et al.

Preparation of Nitro-Phenothiazine Based Oxime Esters (OXEs) as Dual Photo/Thermal Initiators for 3D Printing

Xiaoxiang Zhang[1,2,3], Xiaotong Peng[4], Di Zhu[4], Yijun Zhang[2,3], Marie Le Dot[2,3], Michael Schmitt[2,3], Fabrice Morlet-Savary[2,3], Pu Xiao[4]*, Frédéric, Dumur[5,*], Jacques Lalevée[2,3]*

[1] Zhongyuan University of Technology School of Textiles, Zhengzhou 450007, China
[2] Université de Haute-Alsace, CNRS, IS2M UMR 7361, F-68100 Mulhouse, France
[3] Université de Strasbourg, France
[4] Research School of Chemistry, Australian National University, Canberra, ACT 2601, Australia
[5] Aix Marseille Univ, CNRS, ICR, UMR 7273, F-13397 Marseille, France

*Correspondence: pu.xiao@anu.edu.au; frederic.dumur@univ-amu.fr; jacques.lalevee@uha.fr

Abstract: Nowadays, photopolymerization has spanned across all academic and industrial applications due to its appealing features such as energy saving, environmentally-friendly polymerization conditions, high monomer conversions, rapid polymerization kinetics and so on. Photoinitiator (PI), as a crucial component of the photoinitiating system (PIS) are capable of interacting with light efficiently, enabling to generate initiating species in mono or multicomponent systems. In this work, 13 phenothiazine-based oxime esters (OXEs) (never reported before) were synthesized and their photoinitiation abilities for the free radical photopolymerization (FRP) of acrylates were examined upon irradiation with LED@405 nm. Parallel to their photochemical reactivities, their abilities to initiate thermal polymerization processes were also investigated. Finally, these OXEs exhibited excellent photo/thermal initiation performances, demonstrating their dual initiation properties. Phenothiazine-based oxime esters can be used as PIs in 3D printing as well as thermal initiator in the manufacturing of carbon fiber composites.

Keywords: photoinitiators; photopolymerization; visible light; free radical polymerization; phenothiazine; oxime esters

1. Introduction

Photopolymerization has drawn more and more attention in the academic fields because it is a low-cost, convenient, low-toxic, environmental-friendly, and energy-saving technology [1,2]. With regard to its numerous advantages, photopolymerization has been widely used in research fields, including dentistry, 3D and 4D printing, coatings and microelectronic fabrications [3-5]. Photoinitiator (PI) is one of the most important key components in photopolymerization as it directly interacts with light, promoting the generation of initiating species. At present and considering the fast development of 3D printing, the design of PIs that can be used under near-UV or visible light irradiation becomes more and more important [5-6]. Indeed, LEDs emitting at 405 nm are presently used in 3D printers. With the aim at increasing 3D printing speed, a number of highly reactive photoinitiating systems have been designed[5-8]. However, many of them were multi-component systems consisting of an organic chromophore (often a dye), an onium salt and/or an amine [9,10]. These combinations can induce photopolymerization process *via* intermolecular electron transfer. Nevertheless, the efficiency of these multicomponent systems is greatly affected by the interaction efficacy existing between the photosensitizer and the different additives [9-10], hence influencing monomer conversions. This issue can be addressed if monocomponent photoinitiating systems are used.[11]

One compound fragmenting system is referred as type I photoinitiator [11-12]. However, most of the Type I PIs only work efficiently under UV light [13-14], and only a few PIs, such as diphenyl (2,4,6-trimethylbenzoyl) phosphine oxide (TPO), phenylbis (2,4,6-trimethylbenzoyl)-phosphine oxide (BAPO) and 2-benzyl-2-(dimethylamino) -1-[4-(4-morpholinyl) phenyl]-1-butanone can be photoexcited with visible light [14]. Therefore, the investigation of new

photoinitiators that can be activated under near-UV or visible light is of great interest [15]. Due to their high photo-reactivities, OXEs have gained increasing interests [11,15,16,17]. Their photoinitiation process consists of two steps: i) homolytic cleavage of the N-O bond and ii) decarboxylation reaction of the aryloxy/alkyloxy radicals. To be a good type I PI, the N-O bond of OXEs must have an efficient cleavage process, and then the active free radicals are generated by decarboxylation [18]. *O*-benzoyl-α-oxooxime (OXE01) and *O*-acetyloxime (OXE02) are two examples of commercial OXE Type I PIs. These structures can be photoexcited by the light around 330 nm, implying that these two structures exhibit low performances when exposed to near-UV light (e.g., LED@385 or 395 nm) or visible light (e.g., LED@405 nm) [19]. Therefore, there is an urgent need to develop effective OXE-based photoinitiators activable under mild photopolymerization conditions upon near-UV/visible light irradiation. Different photoinitiators based on other chromophores or wavelengths are also under development [20-21].

In our previous works, a number of OXEs with absorption maxima around 360 nm were proposed as photoinitiators and could be activated in the UV-visible range [22,23]. Photoinitiation and thermal initiation abilities of these OXEs in trimethylolpropane triacrylate (TMPTA) were evaluated, and some of them furnished excellent monomer conversions and could achieve outstanding performance in direct laser write (DLW) experiments. These results motivated us to investigate and expand the family of OXEs that can cater to the demands of various applications of photopolymerization [22-24]. In the present work, a series of nitrophenothiazine-based OXEs exhibiting a dual photo/thermal initiator behavior were presented and discussed.

As shown in Scheme 1, thirteen nitrophenothiazine-based OXEs (from OXE-A to OXE-M) and the same chromophore without the oxime-ester moiety (OXE-N) were developed and synthesized in this study. Since the absorption of phenothiazine derivatives is located in the visible range, phenothiazine was employed as the chromophore in this investigation [25]. In order to improve the absorption in the

visible range, a nitro group was connected to the phenothiazine core. For comparisons, OXE01 and OXE02 were used as benchmark photoinitiators. The chemical structures of the multifunctional monomer TMPTA and the benchmark PIs (OXE01 and OXE02) are shown in Scheme 2. Additionally, photoinitiation abilities and photophysical properties of the different OXEs were investigated using real-time Fourier transformed infrared (RT-FTIR), UV-visible absorption and electron spin resonance spin trapping (ESR-ST). Afterwards, direct laser write experiments were carried out to evaluate their future applications. Markedly, several OXEs demonstrated thermal initiation abilities through differential scanning calorimetry (DSC) analysis, and their corresponding fiber-filled composites were also successfully prepared *via* thermal polymerization coupled with photoinitiation for good curing of the top surface.

2. Results and Discussion

2.1. Synthesis of phenothiazine-based oxime esters

Thirteen nitro-phenothiazine-based oxime esters never reported before were prepared in this work in five steps starting from phenothiazine. Firstly, by alkylation of phenothiazine with iodomethane in the presence of a base, 10-methyl-10*H*-phenothiazine was obtained in 98% yield. Then, by Vilsmeier Haak reaction in 1,2-dichloroethane as the solvent, 10-methyl-10*H*-phenothiazine-3-carbaldehyde was prepared in 82% yield. Nitration of phenothiazine using fuming nitric acid as the nitration agent in acetic acid furnished the targeted 10-methyl-7-nitro-10*H*-phenothiazine-3-carbaldehyde in 68% yield. 10-Methyl-7-nitro-10*H*-phenothiazine-3-carbaldehyde oxime was prepared in quantitative yield using hydroxylamine hydrochloride and sodium acetate using a mixture of solvents. Finally, oxime esters A-M were obtained by esterification of oxime with the appropriate acid chlorides using triethylamine as the base (See Scheme 1). The different oxime esters were obtained with reaction yields ranging from 70% for H to 89% for G (See supporting information, S1.1.1-S1.1.17 and Table S1).

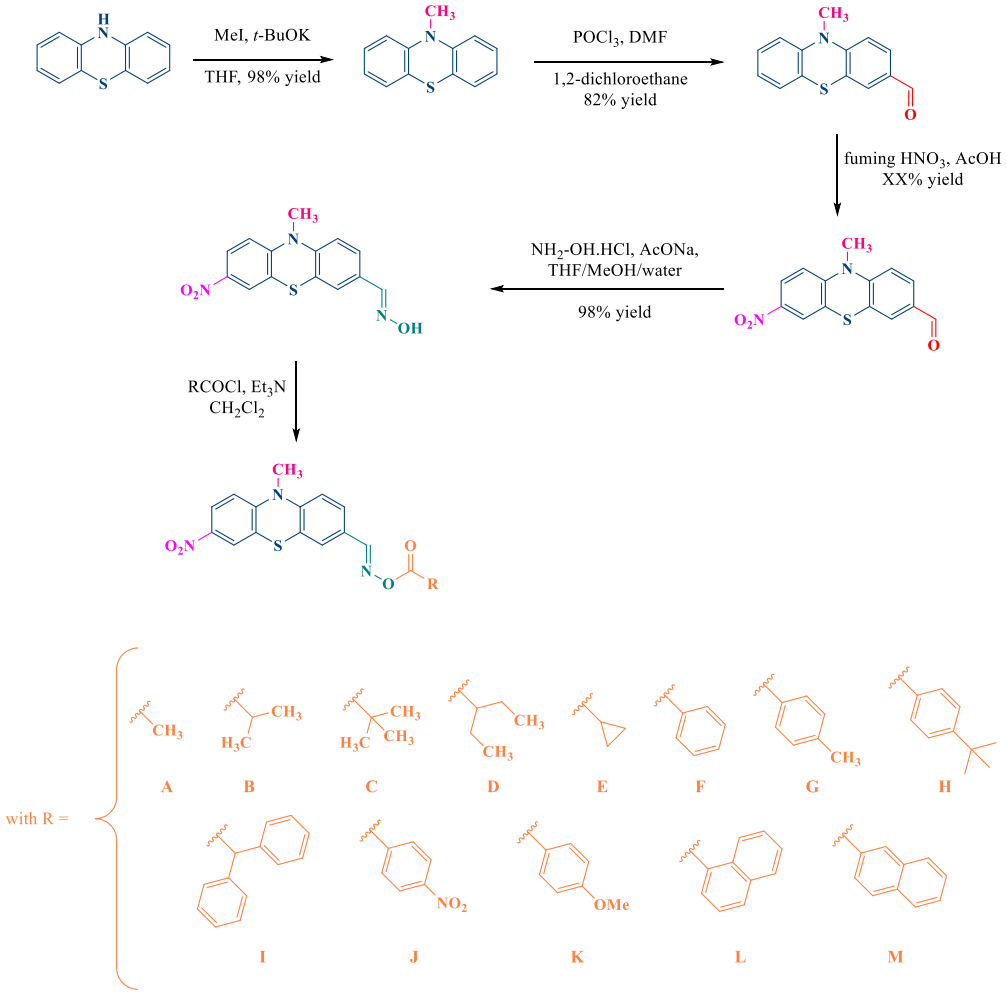
MeI, t-BuOK
THF, 98% yield
POCl3, DMF
1,2-dichloroethane
82% yield
fuming HNO3, AcOH
XX% yield
NH2-OH.HCl, AcONa,
THF/MeOH/water
98% yield
RCOCl, Et3N
CH2Cl2
with R =
A
B
C
D
E
F
G
H
I
J
K
L
M

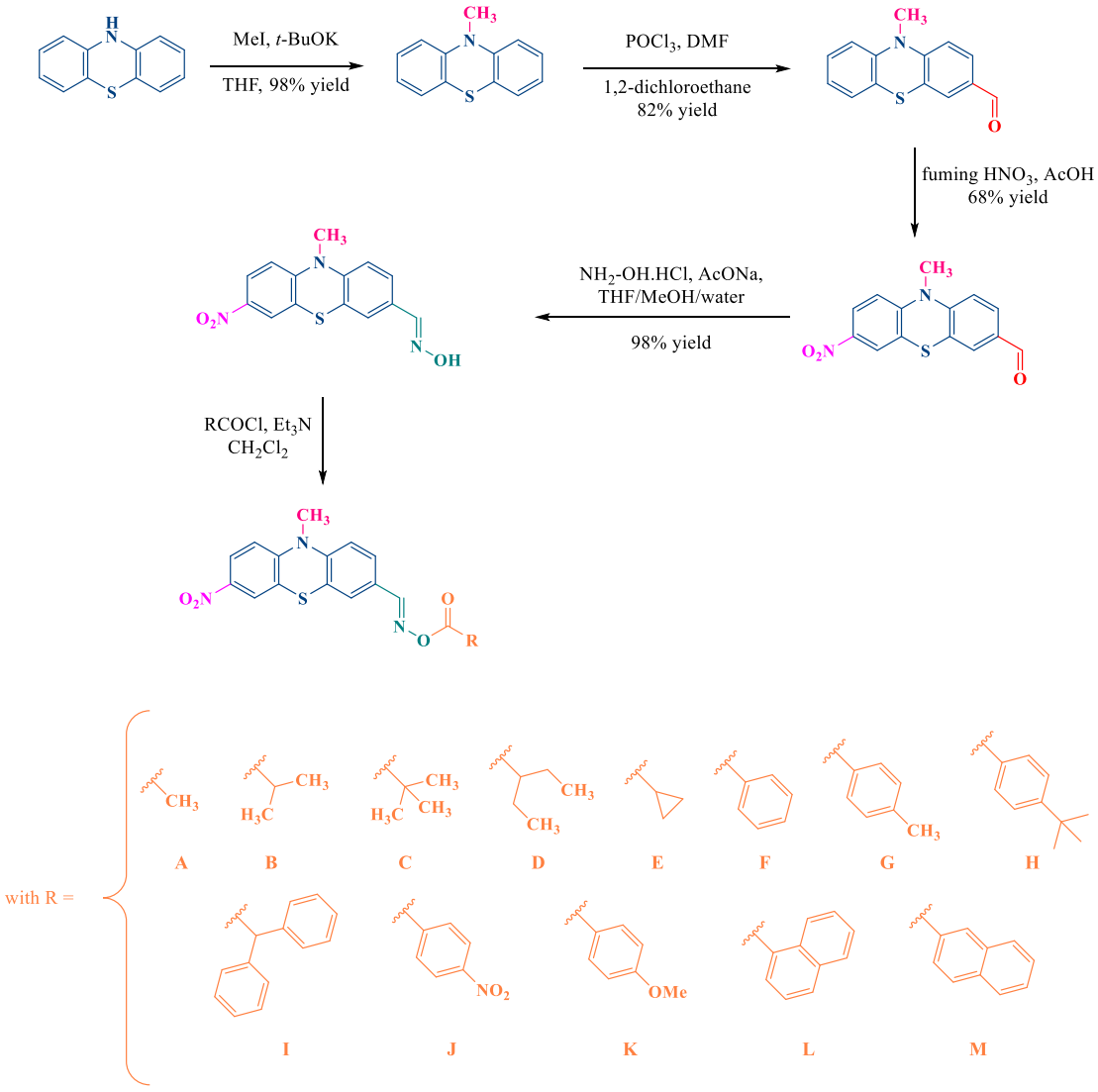

Scheme 1. Synthetic routes of oxime esters (noted OXE-A to OXE-M).

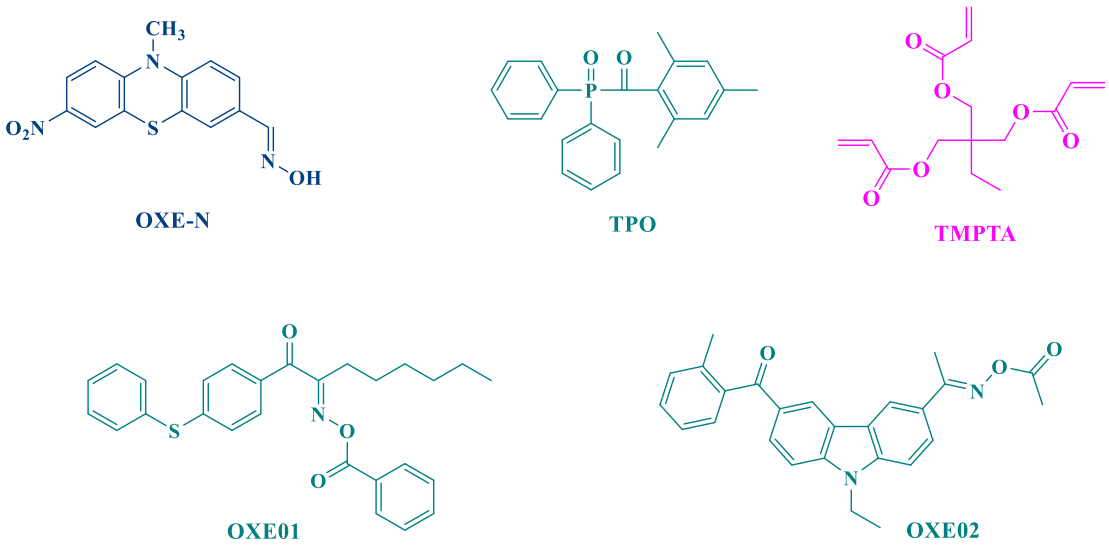

Scheme 2. Chemical structures of OXE-N (the benchmark chromophore without ester

cleavable group), OXE01, OXE02, TPO and TMPTA

2.2. Light Absorption Properties of the Examined OXEs

UV–visible absorption spectra of these investigated OXEs are shown in Figure 1, and the molar extinction coefficients of OXEs are summarized in Table 1. The maximum molar extinction coefficient (ε_{max}) of OXE-N is 2.2×10^4 L/(mol·cm), and its maximum absorption wavelength (λ_{max}) is 376 nm. Compared to OXE-N, the other OXEs have a slight hypsochromic shift in absorbance, as well as lower ε_{max} values. OXE-M had the smallest ε_{max}, which is about 1.1×10^4 L/(mol·cm) at 372 nm. The absorption spectra of these OXEs overlapped with the emission spectrum of the near-UV (405 nm). Hence, these OXEs have the potential to be visible light (LED@405 nm) sensitive photoinitiators.

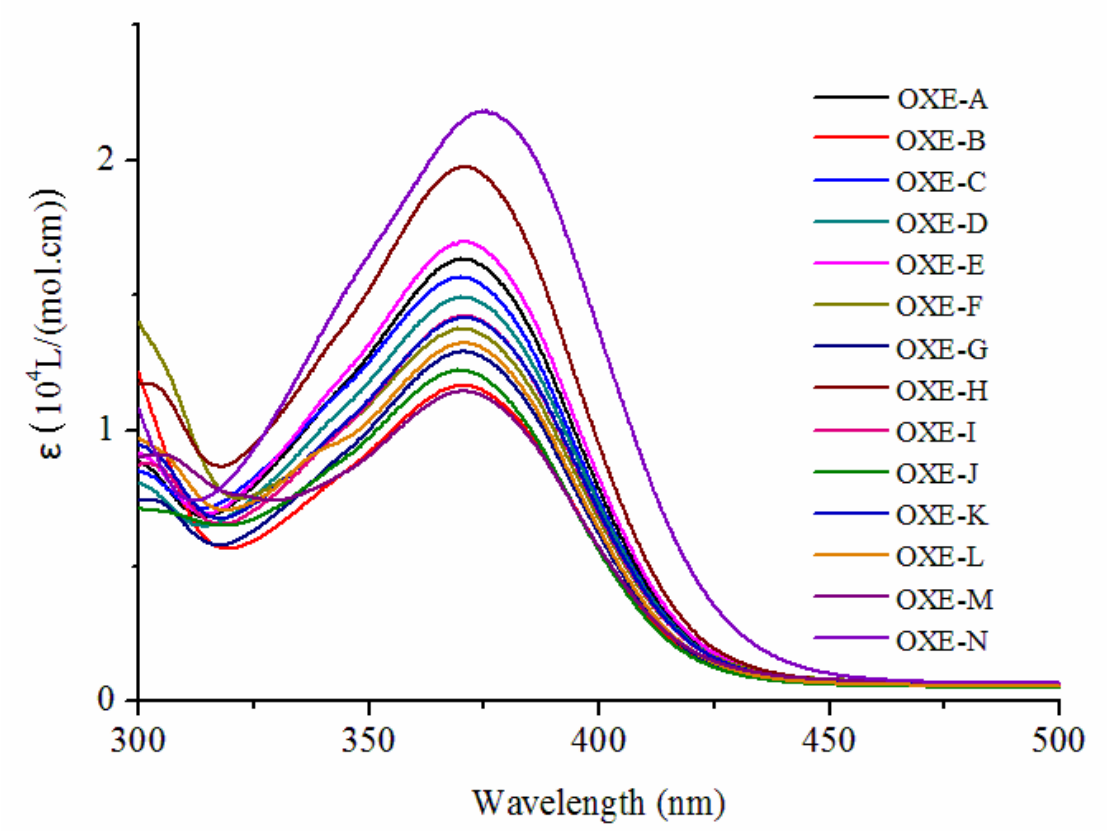

Figure 1. UV-Visible absorption spectra of the different OXEs in acetonitrile (1×10^{-4} mol/L)

Table 1. Absorption characteristics of OXE A-M in acetonitrile (10^{-4} mol/L)

Compounds	**A**	**B**	**C**	**D**	**E**	**F**	**G**
λ_{max} (nm)	371	370	370	370	371	371	371
ε_{max} (10^4L/(mol·cm))	1.65	1.2	1.55	1.5	1.7	1.4	1.3
Compounds	**H**	**I**	**J**	**K**	**L**	**M**	**N**
λ_{max} (nm)	372	372	372	372	373	372	376
ε_{max} (10^4L/(mol·cm))	2.0	1.4	1.2	1.4	1.3	1.1	2.2

2.3. Photoinitiation abilities of OXEs

Polymerization profiles obtained with the different OXEs are given in Figure 2. Interestingly, OXE-N without a cleavable group only showed weak photoinitiation ability and final conversion of 26% was obtained. Other OXEs showed variable photoinitiation abilities during the polymerization of TMPTA. Remarkably, OXE-A has the highest final function conversion (FC = 65%), which is very close to the reference TPO (FC = 69%, the same molecular amount of TPO as a reference/benchmark structure). OXE-J possessing a strong electron-withdrawing group (i.e., a nitrophenyl group) showed only a low final monomer conversion (FC = 40%). It was proposed that cleavage can occur more easily in OXEs with electrophilic groups than in other OXEs [26]. All OXEs containing an oxime ester group bearing an aromatic ring did not achieve high FCs as evidenced by OXE-F (48%), OXE-G (50%), OXE-H (54%), OXE-I (46%), OXE-K (49%), OXE-L (53%) and OXE-M (48%). The steric hindrance effect and the decarboxylation ability [16-17,22-23] also played a relevant role in the initiating performance. This point is notably evidenced by comparing the final monomer conversions obtained with OXE-A, OXE-B and OXE-C. Thus, the FC of OXE-A is higher than that of OXE-B (62%) and OXE-C (57%).

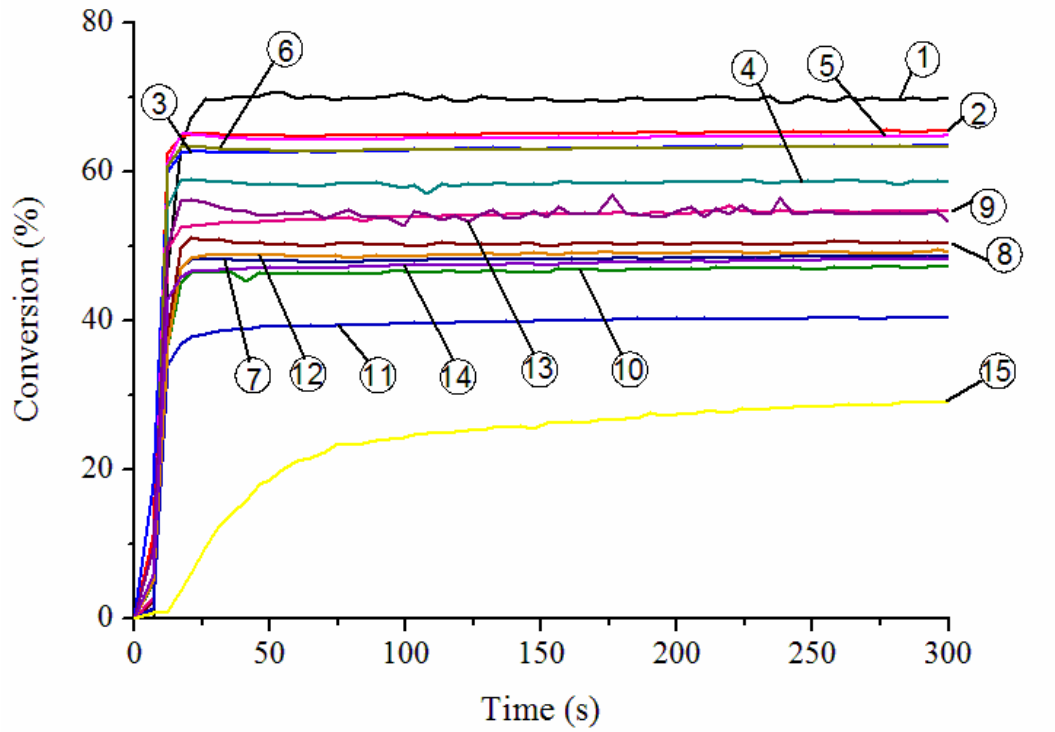

Figure 2. Photopolymerization profiles of TMPTA (acrylate functions conversion vs. time) obtained in laminate (≈ 25 μm) in the presence of OXEs-based PIs (1×10^{-5} mol/g) and TPO (1×10^{-5} mol/g) under LED@405 nm irradiation:
① TPO ② OXE-A ③ OXE-B ④ OXE-C ⑤ OXE-D ⑥ OXE-E ⑦ OXE-F ⑧ OXE-G ⑨ OXE-H ⑩ OXE-I ⑪ OXE-J ⑫ OXE-K ⑬ OXE-L ⑭ OXE-M ⑮ OXE-N.

In order to evaluate the photochemical properties of these OXEs, steady-state photolysis measurements were carried out at room temperature (See Figure 3 and Figure S1-5). As shown in Figure 3, the maximal absorbance of OXE-A decreased upon irradiation at 405 nm during the first 30 s. Meanwhile, new compounds were generated during the photolysis process, as revealed by the hypsochromic shift detected for the maximum absorption wavelength. When exposed to the LED@405 nm, RCOO• radicals are generated by homolytic cleavage of OXEs, which can be detected by ESR (electron spin resonance, See Figure 4). After 30-s irradiation, the hyperfine coupling constants of the main radical adduct (81.0%) were α_N = 13.5 G and α_H =1.8 G which were identified as being an acetoxy radical (CH_3COO•). These hyperfine coupling constants are in full agreement with the literature data [22,27].

These active species can quickly undergo a decarboxylation reaction by releasing CO_2 and create active R• radicals, which can induce a polymerization process.

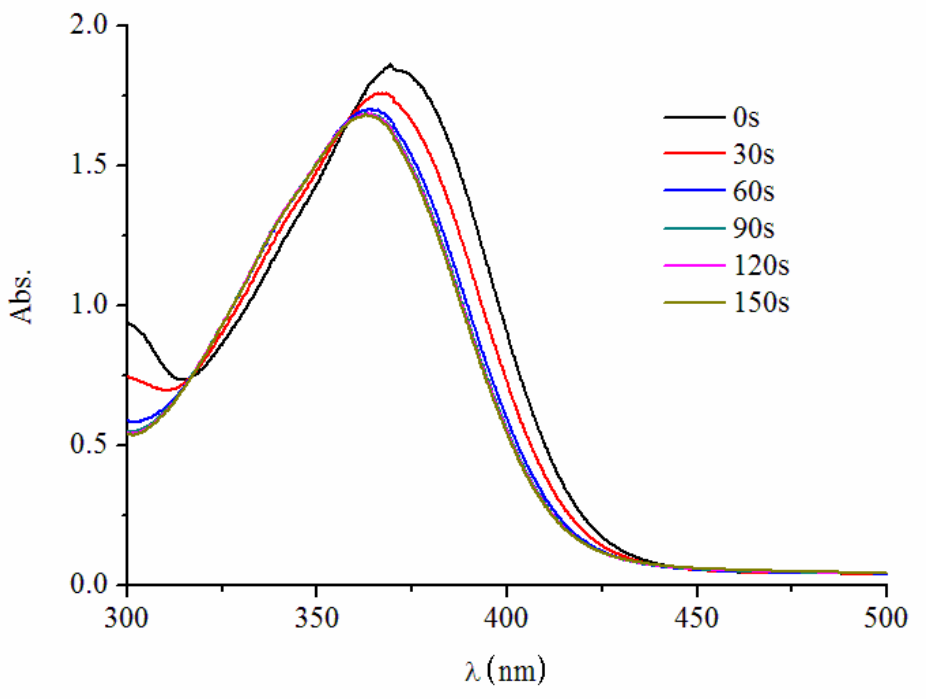

Figure 3. Steady-state photolysis of OXE-A upon irradiation at 405 nm in acetonitrile (1×10^{-4} mol/L).

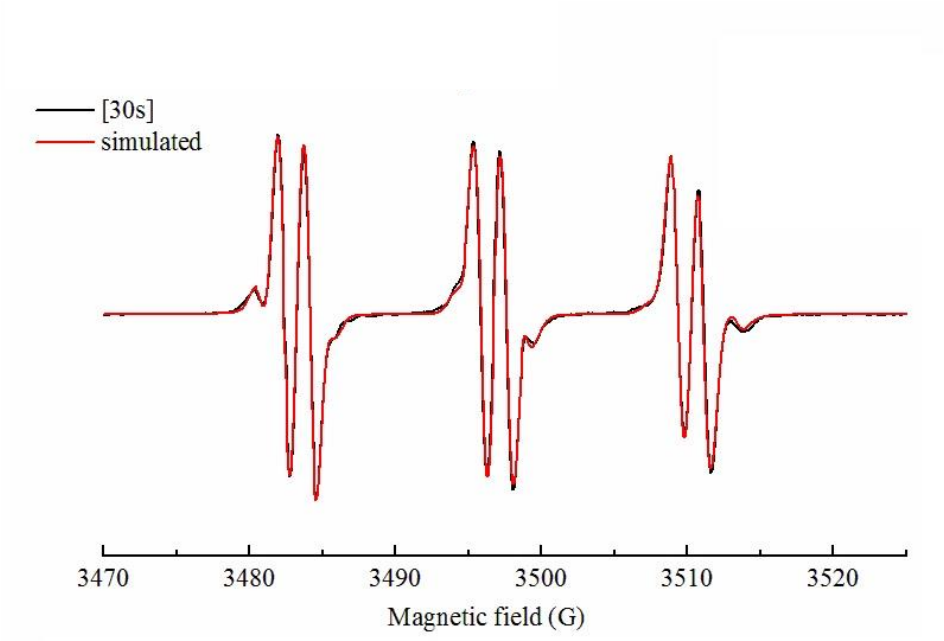

Figure 4. ESR spectrum of OXE-A under irradiation of LED@405 nm (after 30 s) in *tert*-butylbenzene（1×10^{-3} mol/L) and PBN (phenyl-*N*-*tert* butyl nitrone).

The release of CO_2 could be detected by FTIR (See Figure 5). Notably, OXE-A exhibited different infrared spectra during the photopolymerization processes at t = 0 s and t = 30 s. The absorption peak at 2337 cm^{-1} was attributed to the generation of CO_2 [28]. Moreover, no peak was observed for TPO and OXE-N upon light irradiation. This proves the generation of CO_2 by nitrophenothiazine-based OXEs when exposed to LED@405 nm. According to these results above, the photoinitiation mechanism of nitrophenothiazine-based OXEs upon light irradiation was proposed and is shown in Scheme 3 [22,29-30].

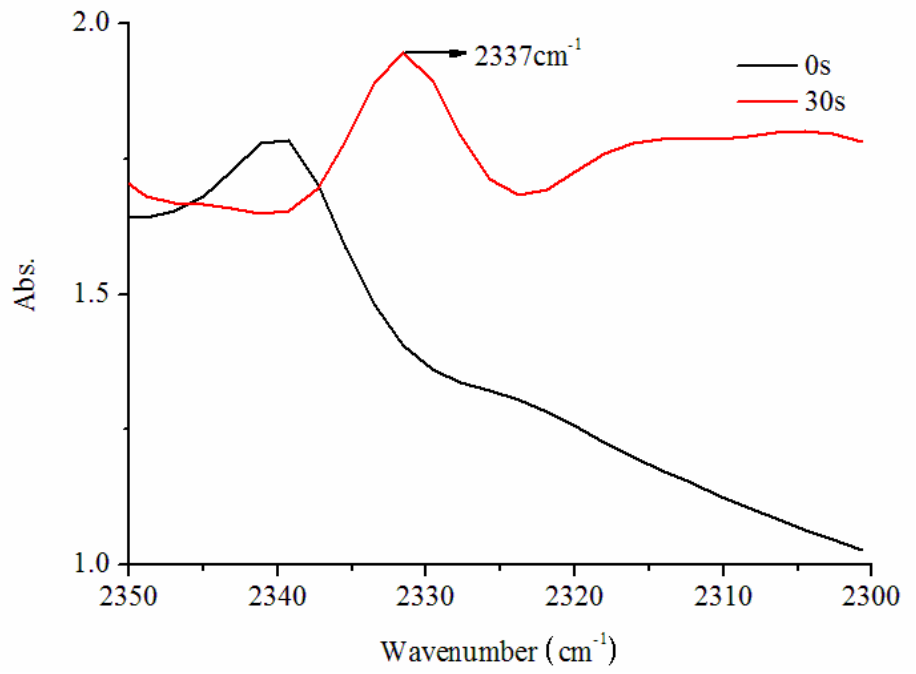

Figure 5. FTIR spectra of TMPTA in the presence of OXE-A (1 × 10^{-5} mol/g) before (black) and after (red) 30-s irradiation of LED@405 nm.

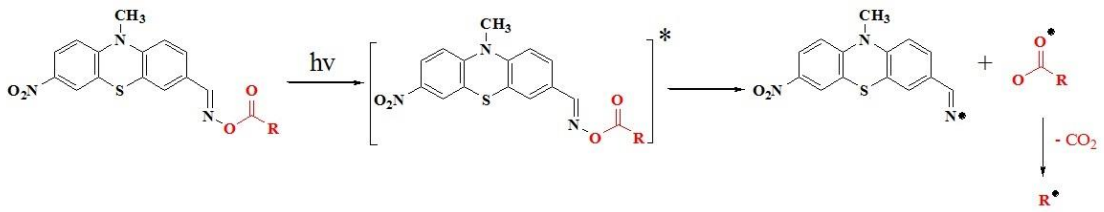

Scheme 3. Proposed mechanism for the photocleavage of nitrophenothiazine-based OXEs.

Upon light exposure, OXEs can be promoted to the excited state, resulting in the dissociation of the N-O bond of OXEs (cleavage reaction) generating acyloxy and imino radicals. Furthermore, acyl radicals can undergo a decarboxylation reaction, and highly reactive radicals (R•) can be generated, promoting the polymerization of acrylate monomers.

2.4. Thermal initiation abilities of OXEs

As reported in previous works, several OXEs-based PIs were found to exhibit dual photo/thermal initiator behaviors [30]. Therefore, this point was examined with the different OXEs reported in this work, and the new proposed OXEs were evaluated for their thermal initiation abilities. Specifically, the thermal initiation abilities of these OXEs in TMPTA were measured by DSC under dark conditions (See Figure 6).

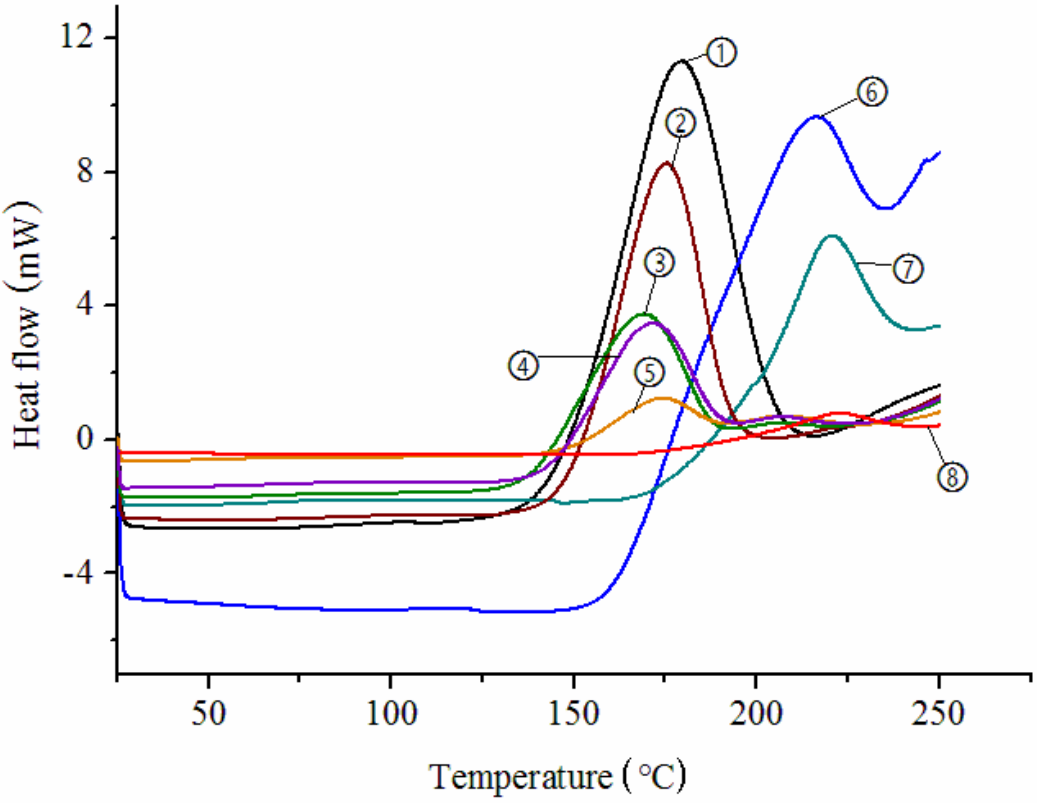

Figure 6. DSC curves of OXEs and TPO in TMPTA (1×10^{-5} mol/g): ① OXE-A ② OXE-E ③ OXE-F ④ OXE-M ⑤ OXE-I ⑥ OXE-N ⑦ TPO ⑧ pure TMPTA (without any initiator).

Compared to pure TMPTA (without OXE or any initiator; Figure 6, curve 8), it is

found that the polymerization can be initiated at lower temperature in presence of OXEs e.g. for OXE-A, the polymerization can be initiated at ~130°C with a maximal temperature ~180°C. This thermal initiating ability of OXE is better than for TPO (curve 7) or the oxime (OXE-N) (curve 6). Thus, OXEs can also be used as a thermal initiator. Details concerning the heating experiments can be found in the supporting information. This dual initiating ability (light and heat) was useful for the curing of opaque samples with: i) a primary fast photopolymerization in the irradiation areas and ii) a secondary curing of the shadow areas by subsequent thermal treatment. An example will be given below.

2.5. Preparation of carbon fiber composite and glass fiber composite

Since most of the carbon fibers are black, the light penetration is thus limited. Therefore, carbon fiber composite materials were usually prepared by thermal curing. In this work, based on its outstanding dual initiation behavior (see above), OXE-A (1×10^{-5} mol/g) was used to prepare carbon fiber composites using TMPTA as the monomer with the following ratio: TMPTA/carbon fiber (50 wt%/ 50 wt%). Due to the limited light penetration inside this black formula, photopolymerization only occurred on the top surface (first step). Thus, the specimen (dimension $100 \times 10 \times 2$ mm) was irradiated with a LED@405 nm up and down for 10 minutes individually. Then, in the second step, the sample was cured in an oven at 150°C for 15 minutes. With the dual-functional initiator, carbon fiber composites were successfully formed as the final product (See Figure 7a). Due to the fact that glass fibers are partly transparent, the glass fiber TMPTA system could be prepared directly by photopolymerization. The same formulation can also be used for the preparation of glass fiber composites upon irradiation with a LED@405 nm for 15 minutes (See Figure 7.b) i.e., only one step is required (the photochemical one).

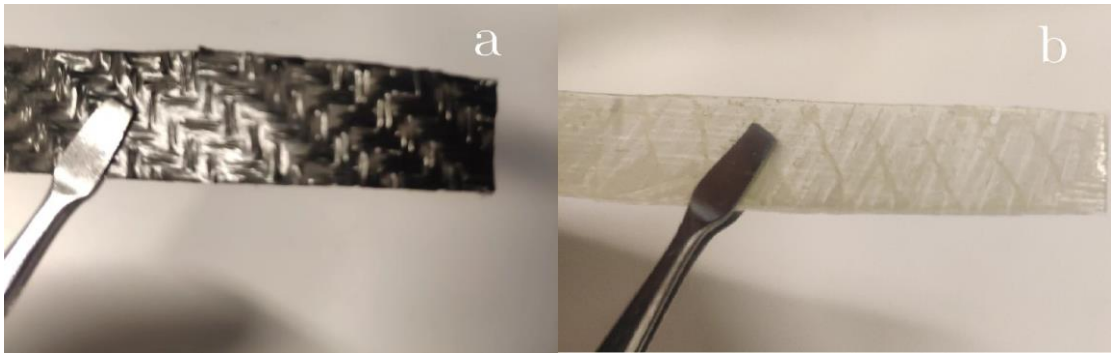

Figure 7. Pictures of (a) carbon fiber composite and (b) glass fiber composite produced using OXE-A (1×10^{-5} mol/g) as a dual photo and thermal initiator.

2.6. Direct Laser Write of the OXE/TMPTA system

Finally, the letter patterns “ZUT” for Zhongyuan University of Technology were written by direct laser write (See Figure 8). A laser diode with an intensity of 110 mW/cm² was used as the irradiation source. OXE-A (1×10^{-5} mol/g) was selected as the photoinitiator, and TMPTA was chosen as the monomer. Some edges of the character were deformed since OXE-A can act as a dual-functional (photo and thermal) initiator where thermal polymerization was taken place at the edge of the laser spot but the spatial resolution remains reasonable. The thickness of the printed pattern letters was about 1770 μm. Remarkably, 3D objects could be easily printed, showing a great prospect for the OXE-A to be used as PI in the future.

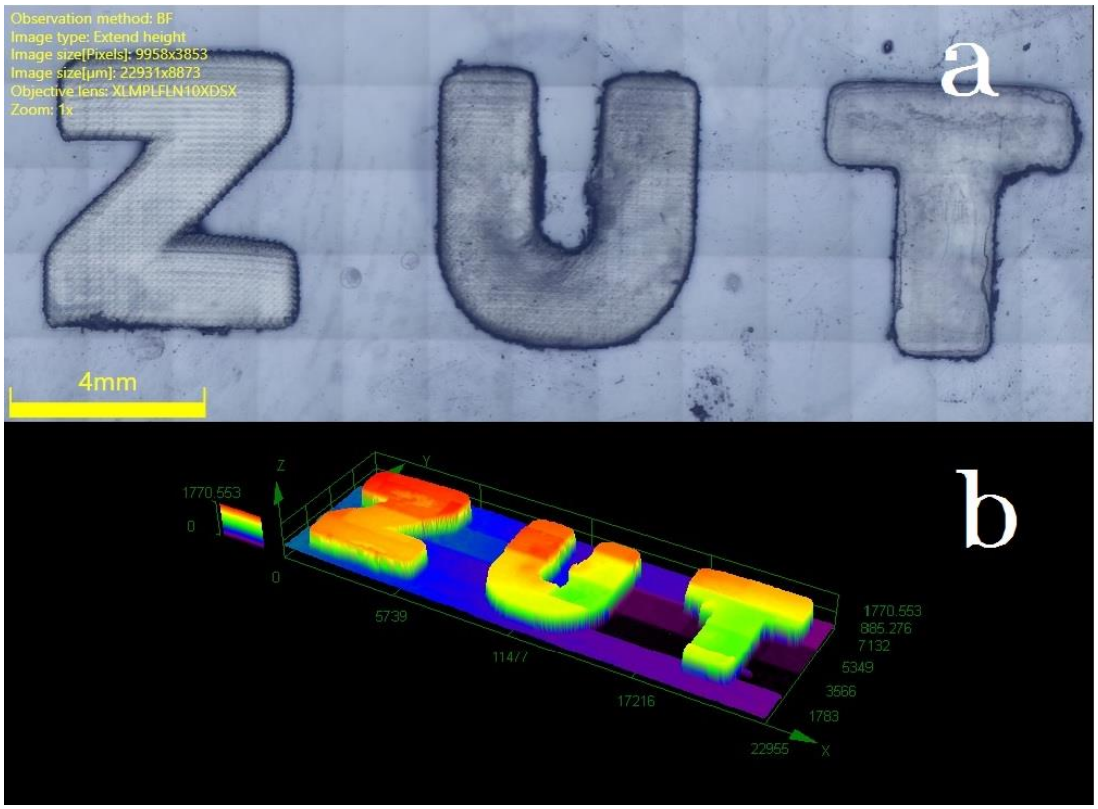

Figure 8. Characterization of the letter pattern "ZUT" by numerical optical microscopy: (a) top surface morphology and (b) 3D overall appearance of the color pattern.

3. Conclusions

In this work, 13 nitrophenothiazine-based OXEs were designed and synthesized as type I photoinitiators for the free radical photopolymerization of TMPTA upon irradiation of LED@405 nm. Their photoinitiation efficiencies were evaluated by RT-FTIR. Specifically, OXE-A achieved the highest final function conversion, thus showing a good photoinitiation efficiency when exposed to LED@405 nm, and exhibiting excellent light absorption properties at this wavelength. Based on its remarkable reactivity, OXE-A could be incorporated in formulations used for direct laser write, enabling to produce 3D letters with a reasonable spatial resolution. Furthermore, the photoinitiating mechanism was revealed by UV-visible absorption spectroscopy, ESR-ST and FTIR. Specifically, the releasing of CO_2 during photopolymerization indicates a photocleavage followed by a decarboxylation process

occurred upon excitation. Therefore, this work reveals the importance of the decarboxylation process in the photoinitiation ability of the different OXEs and provides an achievable strategy for the development of novel and high-performance photoinitiators. Alternatively, their thermal stability and thermal initiation abilities were confirmed by DSC. OXE-A displayed a good dual photo/thermal initiation ability, broadening its potential applications in industries.

Acknowledgments: This research project is supported by China Scholarship Council (CSC No. 201902425004).

References

1. Xiao, P.; Zhang, J.; Dumur, F.; Tehfe, M.-A.; Morlet-Savary, F.; Grff, B.; Gigmes, D.; Fouassier, J.-P.; Lalevée, J. Visible light sensitive Photoinitiating systems: Recent progress in cationic and radical photopolymerization reactions under soft conditions. *Prog. Polym. Sci.* **2015**, 41, 32–66. [CrossRef]
2. Bonardi, A.-H.; Morlet-Savary, F.; Grant, T.M.; Dumur, F.; Noirbent, G.; Gigmes, D.; Lessard, B.H.; Fouassier, J.-P.; Lalevée, J. High performance near-infrared (NIR) photoinitiating systems operating under low light intensity and in presence of oxygen. *Macromolecules* **2018**, 51, 1314–1324. [CrossRef]
3. Lalevée, J.; Blanchard, N.; Tehfe, M.A.; Morlet-Savary, F.; Fouassier, J.P. Green Bulb Light Source Induced Epoxy Cationic Polymerization under Air Using Tris(2,2'-bipyridine)ruthenium(II) and Silyl Radicals. *Macromolecules* **2010**, 43, 10191–10195.
4. Moran, M. J.; Magrini, M.; Walba, D. M.; Aprahamian, I. Driving a liquid crystal phase transition using a photochromic hydrazone. *J. Am. Chem. Soc*. **2018**, 140, 13623–13627. [CrossRef] [PubMed]
5. Mousawi, A. A.; Dumur, F.; Garra, P.; Toufaily, J.; Hamieh, T.; Graff, B.; Gigmes, D.; Fouassier, J.-P.; Lalevée, J. Carbazole Scaffold Based Photoinitiator/Photoredox Catalysts: Toward New High-Performance Photoinitiating Systems and Application in LED Projector 3D Printing Resins. *Macromolecules* **2017**, 50, 2747–2758. [CrossRef]
6. Xiao, P.; Frigoli, M.; Dumur, F.; Graff, B.; Fouassier, J.P.; Gigmes, D.; Lalevée, J. Julolidine or Fluorenone Based Push-Pull Dyes for Polymerization upon Soft Polychromatic Visible Light or Green Light. *Macromolecules.* **2014**, 47, 106–112.
7. Kocaarslan, A.; Kütahya, C.; Keil, D.; Yagci, Y.; Strehmel, B. Near-IR and UV-LED Sensitized Photopolymerization with Onium Salts Comprising Anions of Different Nucleophilicities. *ChemPhotoChem*. **2019**, 3, 1127–1132.
8. Zuo, X.; Morlet-Savary, F.; Schmitt, M.; Le Nouën, D.; Blanchard, N.; Goddard, J.-P.; Lalevée, J. Novel applications of fluorescent brighteners in aqueous visible-light

photopolymerization: high performance water-based coating and LED-assisted hydrogel synthesis. *Polym. Chem*. **2018**, 9, 3952–3958. [Google Scholar] [CrossRef]

9. Lalevée, J.; Telitel, S.; Xiao, P.; Lepeltier, M.; Dumur, F.; Morlet-Savary, F.; Gigmes, D.; Fouassier, J.P. Metal and metal-free photocatalysts: mechanistic approach and application as photoinitiators of photopolymerization. Beilstein *J. Org. Chem*. **2014**, 10, 863–876.
10. Lalevée, J.; Fouassier, J.P. Recent advances in sunlight induced polymerization: Role of new photoinitiating systems based on the silyl radical chemistry. *Polym. Chem*. **2011**, 2, 1107–1113.
11. Zhiquan, L.; Xiucheng, Z.; Guigang, Z.; Xiaoya L.; Ren, Liu. Coumarin-Based Oxime Esters: Photobleachable and Versatile Unimolecular Initiators for Acrylate and Thiol-Based Click Photopolymerization under Visible Light-Emitting Diode Light Irradiation. *Appl. Mater. Interfaces*. **2018**, 9, 16113-16123.
12. Allonas, X.; Morlet, F.; Lalevee, J.; Fouassier, J.P. A photodissociation reaction: experimental and computational study of 2-hydroxy-2,2 dimethylacetophenone. *Photochem. Photobiol.* **2006,** 82, 88–94.
13. Bagheri, A.; Jianyong, J. Photopolymerization in 3D printing. *ACS . Appl. Polym. Mater*. **2019**, 1, 593–611.
14. Dietlin, C.; Schweizer, S.; Xiao, P.; Zhang, J.; Morlet-Savary, F.; Graff, B.; Fouassier, J.-P.; Lalevée, J. Photopolymerization upon LEDs: New Photoinitiating Systems and Strategies. *Polym. Chem*. **2015**, 6, 3895–3912. [CrossRef]
15. Heng, J.; Xiaode, A.; Kun, T.; Tianyi, Z.; Yan, Z.; Shouyun, Y. Visible-light-promoted iminyl-radical formation from acyl oximes: a unified approach to pyridines, quinolines, and phenanthridines. *Angew. Chem. Int. Ed*. **2015**, 54, 4055–4059.
16. Lee, Z.-H.; Hammoud, F.; Hijazi, A.; Graff, B.; Lalevée, J.; Chen, Y.-C. Synthesis and free radical photopolymerization of triphenylamine-based oxime ester photoinitiators. *Polym. Chem.* **2021**, 12, 1286-1297.
17. Hammoud, F.; Lee, Z.H.; Graff, B.; Hijazi, A.; Lalevee, J.; Chen, Y.C. Novel phenylamine-based oxime ester photoinitiators for LED-induced free radical, cationic, and hybrid polymerization. *J. Polym. Sci.* **2021**, 59, 1711–1723.
18. Mallavia, R.; Sastre, R.; Amat-Guerri, F. Photofragmentation and photoisomerization of O-acyl-α-oxooximes: Quantum yields and mechanism, *J. Photochem. Photobiol. A.* **2001**, 138 193–201.
19. David, E. F.; Andrea, L.; Jan, P. M.; Kelterer, A.; Gescheidt, G.; Christopher, B. K. Wavelength-Dependent Photochemistry of Oxime Ester Photoinitiators. *Macromolecules.* **2017**, 50, 1815-1823.
20. Rahal, M.; Mokbel, H.; Graff, B.; Toufaily, J.; Hamieh, T.; Dumur, F.; Lalevée, J. Mono vs. Difunctional Coumarin as Photoinitiators in Photocomposite Synthesis and 3D Printing. *Catalyst.* **2020**, 10, 1202. [CrossRef]
21. Bonardi, A-H.; Bonardi, F.; Noirbent, G.; Dumur, F.; Gigmes, D.; Dietlin, C.; Lalevée, J. Free radical polymerization upon near-infrared light irradiation, merging photochemical and photothermal initiating methods. *J. Polym. Sci*. **2020**, 58, 300–308. [CrossRef]
22. F Hammoud, A Hijazi, M Schmitt, F Dumur, J Lalevee,
A review on recently proposed oxime ester photoinitiators
Eur. Polym. J., **188**, 111901 (2023)

DOI: 10.1016/j.eurpolymj.2023.111901

23. F Hammoud, N Giacoletto, M Nechab, B Graff, A Hijazi, F Dumur, J Lalevee, *5,12-Dialkyl-5,12-dihydroindolo[3,2-a]carbazole-based oxime-esters for LED photoinitiating systems and application on 3D printing* Macromol. Mater. Eng., **307**, 2200082 (2022)
24. Miyake, Y.；Takahashi, H.；Akai, N.；Shibuya, K.；Kawai, A. Structure and Reactivity of Radicals Produced by Photocleavage of Oxime Ester Compounds Studied by Time resolved Electron Paramagnetic Resonance Spectroscopy. *Chem. Lett.* **2014**, 43, 1275–1277.
25. Mahmood, A.; Khan, S.D.; Rana, U. A. Red shifting of absorption maxima of phenothiazine based dyes by incorporating electron-deficient thiadiazole derivatives as π-spacer. *Arab. J. of Chem*. **2019**, 12, 1447-1453.
26. Jiang, H. M.; Zhao, Y. L.; Sun, Q.; Ouyang, X. H.; Li, J. H. Recent Advances in N-O Bond Cleavage of Oximes and Hydroxylamines to Construct N-Heterocycle. *Molecules*. **2023**, 28, 4, 1775.
27. Glen, A.; Russell.; Jerrold, P.; Lokensgard. Application of electron spin resonance spectroscopy to problems of structure and conformation. X. .alpha.-Oxo radicals. *J Am Chem Soc*. **1967**, 19, 5059–5060.
28. Jitendra, Kumar.; Souza, S. F. D. Preparation of PVA membrane for immobilization of GOD for glucose biosensor. *Talanta*. **2008**, 75, 183-188.
29. Lee, Z. H.; Yen, S. C.; Hammoud, F. Naphthalene-Based Oxime Esters as Type I Photoinitiators for Free Radical Photopolymerization. *Polymer*. **2022**, 14, 5261.
30. Shaohui, L.; Pu, X.; Dumur, F,; Lalevée, J. Nitro-Carbazole Based Oxime Esters as Dual Photo/Thermal Initiators for 3D Printing and Composite Preparation. *Macromol. Rapid. Commun*. **2021**, 10, 207–213.